Please open this file and put an X before the desired Mini-Symposia
6 th International Symposium on Solid Mechanics

Select the box to select the Mini-Symposia:

[ ] Multiaxial and Fretting Fatigue (Edgar Mamiya and Lucival Malcher);

[ ] Composite Materials (Ricardo de Medeiros);

[X] Constitutive Models I - Plasticity and Damage (Lucival Malcher, Miguel Vaz Jr. and Edgar Mamiya);

[X] Constitutive Models II - Viscoelastic and Viscoplastic Solids: Models and Applications (Heraldo Mattos);

[ ] Impact Engineering (Marcílio Alves);

[ ] Structural Reliability Methods and Reliability-Based Design Optimization (André Beck);

[ ] Topology Optimization of Multifunctional Materials, Fluids and Structures (Eduardo Lenz Cardoso e Emilio Carlos Nelli Silva);

[ ] Topological Derivatives: Theory and Applications (André Novotny);

[ ] X-FEM, G-FEM and Meshfree Methods (Roberto Dalledone Machado and Rodrigo Rossi);

[ ] High Order Finite Elements (Marco Lúcio Bittencourt);

[ ] Nonlinear Analyses (Eduardo Campello);

[ ] Other section;

MECSOL Joinville 2017

MecSol 2017 – 6th International Symposium on Solid Mechanics

Joinville, SC - Brazil, April 26-28, 2016

ON A DUCTILE-CHEMICAL DAMAGE MODEL FOR BIOABSORBABLE POLYMERIC MATERIALS

Paulo Bastos de Castro[1], Eduardo Alberto Fancello[1] *

[1]Mechanical Engineering Department, Federal University of Santa Catarina, Florianópolis, Santa Catarina, Brazil

*Corresponding author: eduardo.fancello@ufsc.br

Abstract: This work describes and evaluates a recently formulated constitutive model for materials with elastic-viscoplastic characteristic response that may undergo plastic-hydrolytic damage. This phenomenological model, which allows for finite kinematics, stands on the framework of variational constitutive updates, having a consistent thermodynamics basis. We focus on the relation between mechanical and chemical phenomena. Despite the complex nature of the processes involved, it is shown the update algorithm follows a simple operational scheme. As engineering materials, to one degree or another, are susceptible to physical and/or chemical degradation, in general, such processes should be prevented or at least predicted in order to determine the lifetime of components and products. Controlled degradation, however, may be desirable when dealing with environmentally-friendly biodegradable materials, or bioabsorbable medical applications. This work aims specially at bioabsorbable materials, which have been used in the production of medical devices (suture anchors, screws, scaffolds, stents etc) employed in trauma and cardiovascular procedures. Some examples demonstrate that the model succeeded in representing the coupling effects of inelastic flow, mechanical and chemical induced damage. Furthermore, a 3D finite element simulation of a stent-like frame highlights the potential usage of this constitutive formulation

in the design of new products made of bioabsorbable materials..

Keywords: variational constitutive updates, viscoplasticity, plastic-hydrolytic damage, finite element analysis.

MECSOL Joinville 2017

April 26-28, 2017
Joinville, Santa Catarina, Brazil

On a ductile-chemical damage model for bioabsorbable polymeric materials

Paulo Bastos de Castro
Department of Mechanical Engineering
Federal University of Santa Catarina, Florianópolis, SC, Brazil
paulo.bastos@posgrad.ufsc.br

Eduardo Alberto Fancello
Department of Mechanical Engineering
Federal University of Santa Catarina, Florianópolis, SC, Brazil
eduardo.fancello@ufsc.br

ABSTRACT

This work describes and evaluates a recently formulated constitutive model for materials with elastic-viscoplastic characteristic response that may undergo plastic-hydrolytic damage. This phenomenological model, which allows for finite kinematics, stands on the framework of variational constitutive updates, having a consistent thermodynamics basis. We focus on the relation between mechanical and chemical phenomena. Despite the complex nature of the processes involved, it is shown the update algorithm follows a simple operational scheme. As engineering materials, to one degree or another, are susceptible to physical and/or chemical degradation, in general, such processes should be prevented or at least predicted in order to determine the lifetime of components and products. Controlled degradation, however, may be desirable when dealing with environmentally-friendly biodegradable materials, or bioabsorbable medical applications. This work aims specially at bioabsorbable materials, which have been used in the production of medical devices (suture anchors, screws, scaffolds, stents etc) employed in trauma and cardiovascular procedures. Some examples demonstrate that the model succeeded in representing the coupling effects of inelastic flow, mechanical and chemical induced damage. Furthermore, a 3D finite element simulation of a stent-like frame highlights the potential usage of this constitutive formulation in the design of new products made of bioabsorbable materials.

Keywords: variational constitutive updates, viscoplasticity, plastic-hydrolytic damage, finite element analysis

1. INTRODUCTION

Bioabsorbable polymeric materials have been widely used in the design and production of medical implants such as interference screws, suture anchors, stents etc. As a consequence of this fact, considerable advances in trauma, orthopedic and cardiovascular procedures have been achieved. These materials have as its hallmark the capacity to degrade once in contact with water, being this a chemical process known as hydrolysis. A controlled hydrolytic process can be employed, for example, when a component implanted into the human body is expected to degrade progressively while it accomplishes its function, then being absorbed and/or eliminated by the organism. Given the importance of this group of materials, a considerable amount of studies has been carried out concerning the chemical and thermo-mechanical behavior of such polymers.

Several works found in the literature have suggested approaches for modeling hydrolytic damaging and other analogous processes. Based on [1], a formulation taking into account the hydrolysis phe-

nomenon in order to describe the response of materials undergoing deformation-induced degradation was proposed by [2, 3]. In such a class of models, some material parameters are taken as function of the degradation state instead of being material constants. Similar approach also appears in [4, 5, 6, 7]. Moreover, constitutive models for hydrolytic degradation that account for concentration and water diffusion are presented in [8, 9, 10]. Additional references on hydrolytic degradation models can be found in works like [11, 12, 13, 14]. In general, these formulations are limited to viscoelasticity models and do not include plastic or viscoplastic characteristic responses, as well as plastic damage effects. A summary of some studies found in the literature is presented in Tables 1 and 2.

In this paper, a model recently formulated [15, 16] that takes into account coupling effects of elasto-viscoplasticity, ductile damage and hydrolytic degradation is briefly presented, and some examples of its representation capabilities are shown. The model is embedded within the so-called variational constitutive framework where incremental stress-deformation relations can be consistently derived from pseudo-elastic strain-energy potentials [17, 18].

Table 1. Selected references (1).

Reference	Finite Kin.	Application	Geometry	Material	Test
[1]	yes				shear, bend
[19]	no	stents	ring		expansion, cyclic
[2]	yes	stents			
[20]	yes	stents	ring,fiber,stent, etc	PLLA	expansion, shear, torsion, tensile
[3]	yes	stents	ring		expansion, tensile
[21]	yes			PLA-PCL	tensile
[4]	yes		fiber	PLA-PCL	tensile
[5]	yes	ligament	rope	PLA-PLC	tensile
[7]	yes			PLA-PCL	tensile
[6]	yes	stents	ring	PLLA	expansion
[22]	yes	soft tissues			tensile (+swelling)
[23]	yes	soft tissues			tensile
[9]	yes		slab		shear
[24]	no		concentric ring		
[10]	yes	stents	concentric ring		
[25]	no		sp d=4mm l=16mm	AISI 304	tensile
[26]	no		spc. d=4mm l=16mm	AISI 304	tensile
[27]	no		spc. d=4mm l=16mm	AISI 304	tensile
[28]		stents		magnesium	expansion stent+artery
[29]		stents		magnesium	expansion stent

Kin. kinematic, sp. test specimen, d. diameter, l. length

Table 2. Selected references (2).

Reference	Var. Updates.	Ductile damage	Visco	Potential	Code
[1]	no	no	no	neo-Hookean	Matlab (ODE113)
[19]	no	no	no	elastic	NLFE
[2]	no	no	no	neo-Hookean	
[20]	no	no	viscoelastic	n-H, M-R, P2nd	NLFE, Abaqus (UMAT)
[3]	no	no	no	Knowles	R-K
[21]	no	no	no	n-H, M-R, P2nd	
[4]	no	no	no	n-H, M-R, P2nd	Abaqus-Python-UMAT
[5]	no	no	no	neo-Hookean	Abaqus-Python-UMAT
[7]	no	no	(viscoelastic)	BB	MCalibration
[6]	yes	no	viscoelastic	Odgen	Abaqus (UMAT)
[22]	no	no	no	n-H + (fibers)	
[23]	no	no	no	n-H + (fibers)	
[9]	no	no			
[24]	no	no	no		Abaqus (UMAT)
[10]	no	no	QLV		Abaqus (UMAT)
[25]	no	yes	yes		
[26]	no	yes	yes		
[27]	no	yes	yes		
[28]	no	no	no		Abaqus (VUMAT)
[29]	no	no	no		Abaqus (VUMAT / VUSDFLD)

Var. updates Variational updates, n-H. neo-Hookean, M-R. Mooney-Rivlin, P2nd. Second order potential, BB. Bergstrom-Boyce, QLV quasi-linear viscoelastic, UMAT/VUMAT. user material (implicit/explicit), NLFE. Nonlinear finite elements, R-K. Runge-Kutta

2. VARIATIONAL CONSTITUTIVE UPDATES

Aiming at the definition of some basic notation, this section outlines the framework proposed by [17, 18]. Let a set of state variables be defined as $\mathscr{E} = \{\mathbf{F}, \mathbf{Z}\}$, where $\mathbf{F}$ is the deformation gradient and $\mathbf{Z}$ represents internal variables associated with dissipative processes. By assuming the existence of a free-energy potential W, which is functionally dependent on $\mathscr{E}$, one has

$$W = W(\mathscr{E}), \qquad \mathbf{P} = \frac{\partial W}{\partial \mathbf{F}}, \qquad \mathbf{Q} = \frac{\partial W}{\partial \mathbf{Z}}. \tag{1}$$

The power $\mathscr{D}$ dissipated by a mechanical process, not considering the thermal effects, is given by the difference between the stress power and the rate of the free-energy [17],

$$\mathscr{D} = \mathbf{P} : \dot{\mathbf{F}} - \dot{W} \geq 0\,. \tag{2}$$

Taking the time derivative of W, substituting it into (2) and by making use of the Coleman-Noll procedure [30], the following condition is attained:

$$\mathscr{D} = -\mathbf{Q} * \dot{\mathbf{Z}} \geq 0, \tag{3}$$

where $*$ represents an appropriate product operation. The equation in (3) provides the power dissipation for a change of the system state and must be non-negative for every thermodynamically consistent model. An effective way of satisfying this inequality is by assuming the existence of a potential $\phi = \phi(Q; \mathscr{E})$, which must be convex, non-negative, zero value at the origin [17] such that $-\dot{\mathbf{Z}} \in \partial\phi(Q)$, where $\partial\phi(\mathbf{Q})$ defines the set of subdifferentials related to $\phi(\mathbf{Q})$. By convexity properties, there exists a convex conjugate function

$$\phi^* = \sup\{-\dot{\mathbf{Z}} * \mathbf{Q} - \phi(\mathbf{Q})\}, \qquad \mathbf{Q} \in \partial\phi^*(-\dot{\mathbf{Z}}), \tag{4}$$

where ϕ^* is the Legendre transform of ϕ. If ϕ^* is Fréchet differentiable, the set $\partial\phi^*(-\dot{Z})$ is reduced to a single derivative element, $\mathbf{Q} = -\frac{\partial\phi^*(\dot{\mathbf{Z}})}{\partial\dot{\mathbf{Z}}}$, which its substitution into (1-c) results in the general evolution equation for the internal variables,

$$\frac{\partial W(\mathbf{Z})}{\partial \mathbf{Z}} + \frac{\partial \phi^*(\dot{\mathbf{Z}})}{\partial \dot{\mathbf{Z}}} = 0. \tag{5}$$

An alternative way of setting the state equations (1-b), (1-c) and the evolution equation (5), in such a fashion that the inequality (3) is satisfied, is achieved by means of the definition of the following potentials

$$\mathscr{P}(\dot{\mathbf{F}}, \dot{\mathbf{Z}}; \mathscr{E}) = \dot{W}(\dot{\mathbf{F}}, \dot{\mathbf{Z}}; \mathscr{E}) + \phi^*(\dot{\mathbf{Z}}; \mathscr{E}) = \frac{\partial W}{\partial \mathbf{F}} : \dot{\mathbf{F}} + \frac{\partial W}{\partial \mathbf{Z}} * \dot{\mathbf{Z}} + \phi^*(\dot{\mathbf{Z}}; \mathscr{E}), \tag{6}$$

$$\bar{\mathscr{P}}(\dot{\mathbf{F}}; \mathscr{E}) = \inf_{\dot{\mathbf{Z}}} \mathscr{P}(\dot{\mathbf{F}}, \dot{\mathbf{Z}}; \mathscr{E}) \, . \tag{7}$$

The optimality condition for the minimization of $\mathscr{P}$ with respect to $\dot{\mathbf{Z}}$ yields the evolution equation (5), while the partial derivative of $\bar{\mathscr{P}}$ with respect to $\dot{\mathbf{F}}$ results in the state equation (1-b),

$$\mathbf{P} = \frac{\partial W}{\partial \mathbf{F}} = \frac{\partial \bar{\mathscr{P}}(\dot{\mathbf{F}}; \mathscr{E})}{\partial \dot{\mathbf{F}}}, \tag{8}$$

that is, $\bar{\mathscr{P}}$ is a potential for $\mathbf{P}$ in terms of the argument $\dot{\mathbf{F}}$.

Since numerical techniques are to be employed, it may be convenient to define incremental constitutive laws which could be obtained by means of discrete time integration of Equation (8). Nonetheless, by following the approach presented by [17, 18], the constitutive updates are achieved by means of extremization procedures involving the incremental potentials

$$\mathscr{W}(\mathbf{F}_{n+1}, \mathbf{Z}_{n+1}; \mathscr{E}_n) = W(\mathbf{F}_{n+1}, \mathbf{Z}_{n+1}) - W(\mathbf{F}_n, \mathbf{Z}_n) + \Delta t \, \phi^*(\mathbf{Z}_{n+1}; \mathscr{E}_n) \, , \tag{9}$$

$$\bar{\mathscr{W}}(\mathbf{F}_{n+1}; \mathscr{E}_n) = \inf_{\mathbf{Z}_{n+1}} \mathscr{W}(\mathbf{F}_{n+1}, \mathbf{Z}_{n+1}; \mathscr{E}_n) \, . \tag{10}$$

having the properties [17]:

1. its minimization with respect to $\mathbf{Z}_{n+1}$ yields the incremental evolution equation for $\mathbf{Z}$

$$\frac{\partial W_{n+1}}{\partial \mathbf{Z}_{n+1}} + \Delta t \frac{\partial \phi^*(\mathbf{Z}_{n+1}; \mathscr{E}_n)}{\partial \mathbf{Z}_{n+1}} = 0 \, ; \tag{11}$$

2. the partial derivative of $\bar{\mathscr{W}}$ with respect to $\mathbf{F}_{n+1}$ results in the expression for the stress tensor update

$$\mathbf{P}_{n+1} = \frac{\partial \bar{\mathscr{W}}}{\partial \mathbf{F}_{n+1}} \, , \tag{12}$$

which can be alternatively written in terms of the right Cauchy-Green deformation tensor $\mathbf{C}_{n+1}$, yielding the second Piola-Kirchhoff stress

$$\mathbf{S}_{n+1} = 2 \frac{\partial \bar{\mathscr{W}}}{\partial \mathbf{C}_{n+1}}. \tag{13}$$

In the next section, this variational approach is employed in order to present an elastic-viscoplastic model that couples mechanical and hydrolytic damage effects.

3. VISCOPLASTIC MODEL WITH PLASTIC-HYDROLYTIC DAMAGE

3.1 Initial considerations

The constitutive model to be presented in this work has been proposed in [15, 16]. For the sake of clearness and completeness, the main features of that formulation is reproduced here. In such a model, the viscoplastic formulation is based on a dissipation function of Perzyna-type. The plastic damaging process resembles the classic Lemaitre's model [31, 32] with a scalar damage internal variable. Additionally, the strain equivalence hypothesis is adopted. Diffusion (and concentration) effects are neglected by assuming that the diffusion time-scale is very much shorter than the degradation itself. The hydrolytic damage evolution follows the model proposed by [33]. All the characteristics previously mentioned are then set in the variational framework established by [17] and [18].

3.2 Model description

By considering a kinematic framework of finite deformations, the classic Kröner-Lee multiplicative decomposition of $\mathbf{F}$ is used, that is

$$\mathbf{F} = \mathbf{F}^e\mathbf{F}^p. \tag{14}$$

The velocity gradient $\mathbf{L} = \dot{\mathbf{F}}\mathbf{F}^{-1}$ is split into its elastic and plastic contributions

$$\mathbf{L} = \mathbf{L}^e + \mathbf{F}^e\mathbf{L}^p(\mathbf{F}^e)^{-1}, \quad \mathbf{L}^e \equiv \dot{\mathbf{F}}^e(\mathbf{F}^e)^{-1}, \quad \mathbf{L}^p \equiv \dot{\mathbf{F}}^p(\mathbf{F}^p)^{-1}. \tag{15}$$

Then, the elastic term $\mathbf{F}^e$ is decomposed into isochoric and volumetric parts, as well as $\mathbf{F}^v$ is assumed to be isochoric (i.e. $\det\mathbf{F}^v \equiv 1$), so

$$\mathbf{F}^e = \hat{\mathbf{F}}^e\mathbf{F}^v\,, \qquad \hat{\mathbf{F}}^e = J^{-\frac{1}{3}}\mathbf{F}^e\,, \qquad \mathbf{F}^v = J^{\frac{1}{3}}\mathbf{I}\,, \qquad \hat{\mathbf{C}}^e = \hat{\mathbf{F}}^{e\,T}\hat{\mathbf{F}}^e, \tag{16}$$

where $\hat{\mathbf{C}}^e$ is the Cauchy-Green isochoric deformation tensor, $J = \det\mathbf{F}$ and $\mathbf{I}$ is the second-order identity tensor.

The set of state variables $\mathscr{E}$ is comprised of the deformation gradient $\mathbf{F}$, the plastic deformation gradient $\mathbf{F}^p$, an internal variable α (equivalent to a measure of the accumulated plastic strain), the plastic damage d^p and the hydrolytic damage d^h:

$$\mathscr{E} = \left\{\mathbf{F}, \mathbf{F}^p, \alpha, d^h, d^p\right\}\,. \tag{17}$$

The free-energy potential W is considered to be linearly dependent on the total damage $d = d^p + d^h$, that is

$$W = (1-d)\left[W^e(\hat{\mathbf{C}}^e) + W^p(\alpha) + U(J)\right]\,, \tag{18}$$

where W^e, W^p e U are respectively related to the isochoric elastic, plastic and volumetric elastic contributions of the free-energy potential. One may notice that all terms of W are affected by the total damage d, which is a main difference between the current approach and the classic Lemaitre's model. Such a proposition was previously noticed in papers such as [34, 35, 36], bringing about a convenient simplification regarding the model and its mathematical formulation as well.

Once defined the free-energy arguments, its time derivative takes the particular form

$$\dot{W} = \frac{\partial W}{\partial \mathbf{F}} : \dot{\mathbf{F}} + \frac{\partial W}{\partial \mathbf{F}^p} : \dot{\mathbf{F}}^p + \frac{\partial W}{\partial \alpha}\dot{\alpha} + \frac{\partial W}{\partial d^p}\dot{d^p} + \frac{\partial W}{\partial d^h}\dot{d^h}, \tag{19}$$

and by considering inequality (2) and the Coleman-Noll procedure, the following conjugate forces are defined:

$$\mathbf{P} = \frac{\partial W}{\partial \mathbf{F}}, \qquad \chi = \frac{\partial W}{\partial \mathbf{F}^p}, \qquad \kappa = \frac{\partial W}{\partial \alpha}, \tag{20}$$

$$-Y^p = \frac{\partial W}{\partial d^p}, \qquad -Y^h = \frac{\partial W}{\partial d^h}. \tag{21}$$

Since $d = d^p + d^h$, the assumption (18) leads to the equality $Y = Y^p = Y^h$.

Two constraints are then enforced between the internal variables. The first one relates $\mathbf{F}^p$ and α by means of the non-holonomic parametrization [17]

$$\mathbf{D}^p = \mathbf{L}^p = \dot{\mathbf{F}}^p \left(\mathbf{F}^p\right)^{-1} = \dot{\alpha}\mathbf{M}\,, \tag{22}$$

$$\mathbf{M} \in \mathscr{K}_{\mathrm{M}} = \left\{ \mathbf{N} \in \mathtt{Sym.}; \mathbf{N} : \mathbf{N} = \frac{3}{2}; \mathbf{N} : \mathbf{I} = 0 \right\}\,, \tag{23}$$

where the usual assumption of a null plastic spin $\mathbf{W}^p = 0$ is employed. The scalar variable $\dot{\alpha} \geq 0$ measures the stretching amplitude, while the tensor $\mathbf{M}$ defines the stretching direction. The second (non-holonomic) constraint associates the plastic damage d^p with α by means of the following evolution law:

$$\dot{d^p} = \dot{\alpha}\frac{Y^S}{N}, \tag{24}$$

where S and N are material constants.

In accordance with the general conditions presented in Section 2, a suitable dissipation function is proposed, being split into viscoplastic, mechanical damage and hydrolytic contributions

$$\phi^* = \psi^*_{vp} + \varphi^*_{dp} + \varphi^*_{dh}\,. \tag{25}$$

The potential ψ^*_{vp} is similar to Perzynas's function:

$$\psi^*_{vp} = \begin{cases} (1-d)\,\sigma_Y\,\dot{\alpha} + \dfrac{\mathtt{c} f_A(\alpha)}{\eta+1}\left(\dfrac{\dot{\alpha}}{\mathtt{c}}\right)^{\eta+1} & \text{if } \dot{\alpha} \geq 0 \\ +\infty & \text{if } \dot{\alpha} < 0 \end{cases}\,, \tag{26}$$

where d is the total damage, σ_Y is the initial yield stress, $f_A(\alpha)$ is a function associated with material viscoplastic saturation [37], and η and $\mathtt{c}$ are material constants.

The plastic damage dissipative function φ^*_{dp} is given by

$$\varphi^*_{dp} = \begin{cases} \dot{d^p} Y = \dot{\alpha}\dfrac{Y^{S+1}}{N} & \text{if } \dot{\alpha} \geq 0 \\ +\infty & \text{if } \dot{\alpha} < 0 \end{cases}\,. \tag{27}$$

Finally, the hydrolytic dissipative function φ^*_{dh} has the form

$$\varphi^*_{dh} = \begin{cases} \dfrac{R}{2\left(1-d\right)^n \left(Y+g\right)^{m-1}}\,\dot{d^h}^{\,2} - g\,\dot{d^h} & \text{if } \dot{d^h} \geq 0 \\ +\infty & \text{if } \dot{d^h} < 0 \end{cases}\,, \tag{28}$$

where R, m, g are material constants. The term $g\dot{d^h}$ guarantees the evolution of d^h even in absence of strain-related energies. It is worth noticing that negative values of $\dot{\alpha}, \dot{d^p}$ and $\dot{d^h}$ are avoided due to exact penalization on the corresponding dissipation functions.

Also, let the effective thermodynamics forces be defined as

$$\tilde{\mathbf{P}} = \frac{\mathbf{P}}{(1-d)}, \qquad \tilde{\chi} = \frac{\chi}{(1-d)}, \qquad \tilde{\kappa} = \frac{\kappa}{(1-d)} \; . \tag{29}$$

By using the definitions (18), (26), (27) and (28) , the pseudo-potentials $\mathscr{P}$ and $\bar{\mathscr{P}}$ take the forms

$$\mathscr{P}(\dot{\mathbf{F}}, \dot{\alpha}, \mathbf{M}, \dot{d^h}; \mathscr{E}) = \dot{W}(\dot{\mathbf{F}}, \dot{\alpha}, \mathbf{M}, \dot{d^h}; \mathscr{E}) + \phi^*(\dot{\alpha}, \dot{d^h}; \mathscr{E}) \; , \tag{30}$$

$$\bar{\mathscr{P}}(\dot{\mathbf{F}}; \mathscr{E}) = \inf_{\dot{\alpha}\geq 0,\, \mathbf{M}\in\mathscr{K}_{\mathrm{M}},\, \dot{d^h}\geq 0} \mathscr{P}(\dot{\mathbf{F}}, \dot{\alpha}, \mathbf{M}, \dot{d^h}; \mathscr{E}) \; . \tag{31}$$

3.3 Incremental update formulation

In order to solve numerically the constitutive problem, an incremental potential consistent with (30) has to be defined. This definition can be performed by assuming initially the following discrete approximations,

$$\dot{\alpha} := \frac{\Delta\alpha}{\Delta t}, \qquad \dot{d} := \frac{\Delta d}{\Delta t}, \qquad \Delta d^p = \Delta\alpha \frac{Y^S}{N}, \tag{32}$$

and then considering the incremental potentials

$$\mathscr{W} = [W(\mathscr{E}_{n+1}) - W(\mathscr{E}_n)] + \Delta t \phi^* \left(\mathbf{M},\, \Delta\alpha,\, \Delta d^h\right) \; , \tag{33}$$

$$\bar{\mathscr{W}}(\mathscr{E}_{n+1}; \mathscr{E}_n) = \inf_{\Delta\alpha\geq 0,\, \mathbf{M}\in\mathscr{K}_{\mathrm{M}},\, \Delta d^h\geq 0} \mathscr{W}(\mathscr{E}_{n+1}; \mathscr{E}_n) \; , \tag{34}$$

where W is given by (18) and ϕ^* is taken here as the incremental version of the dissipative potential (25), that after convenient changes in its arguments results in

$$\begin{aligned} \phi^* = {} & (1-d_{n+1})\,\sigma_Y \frac{\Delta\alpha}{\Delta t} + \frac{\mathsf{c} f_A(\alpha_{n+1})}{\eta+1} \left(\frac{\Delta\alpha/\Delta t}{\mathsf{c}}\right)^{\eta+1} \\ & + Y_{n+1} \frac{\Delta d^p}{\Delta t} + \frac{R}{2\,(1-d_{n+\theta})^n \left(Y_{n+\gamma}+g\right)^{m-1}} \left(\frac{\Delta d^h}{\Delta t}\right)^2 - g\frac{\Delta d^h}{\Delta t} \; . \end{aligned} \tag{35}$$

where $d_{n+\theta} = d_n + \theta\left(\Delta\alpha \frac{(Y_{n+\theta})^S}{N} + \Delta d^h\right)$ with $\theta \in [0,1]$, and $Y_{n+\gamma} = \gamma Y_{n+1} + (1-\gamma) Y_n$ with $\gamma \in [0,1]$.

Moreover, $\dot{\mathbf{F}}^p = \mathbf{D}^p \mathbf{F}^p$ is evaluated by means of the exponential mapping [38],

$$\mathbf{F}^p_{n+1} = \exp\left[\Delta t \mathbf{D}^p\right] \mathbf{F}^p_n = \exp\left[\Delta\alpha \mathbf{M}\right] \mathbf{F}^p_n \; . \tag{36}$$

And other useful relations between the elastic and plastic deformations are

$$\hat{\mathbf{F}}^e_{n+1} = \hat{\mathbf{F}}_{n+1} \hat{\mathbf{F}}^{p-1}_{n+1} \tag{37}$$

$$\hat{\mathbf{C}}^e_{n+1} = \hat{\mathbf{F}}^{eT}_{n+1} \hat{\mathbf{F}}^e_{n+1} = \hat{\mathbf{C}}^{pr}_{n+1} \left[\exp\left(\Delta\alpha \mathbf{M}\right)\right]^{-2} \tag{38}$$

$$\hat{\mathbf{C}}^{pr}_{n+1} = \hat{\mathbf{F}}^{p-T}_n \hat{\mathbf{C}}_{n+1} \hat{\mathbf{F}}^{p-1}_n, \tag{39}$$

$$\hat{\varepsilon}^e_{n+1} = \tfrac{1}{2} \ln \hat{\mathbf{C}}^e_{n+1} = \varepsilon^{pr}_{n+1} - \Delta t \mathbf{D}^p \tag{40}$$

$$\varepsilon^{pr}_{n+1} = \tfrac{1}{2} \ln \hat{\mathbf{C}}^{pr}_{n+1} \tag{41}$$

where $(\bullet)^{pr}$indicates predictor quantities. Equation (38) is valid only if $\hat{\mathbf{C}}^{pr}$and $\mathbf{D}^p$are assumed colinear, allowing permutation between both tensors [39, 40].

The minimization with respect the tensor $\mathbf{M}$ is performed by means of a Lagrangian function. It is shown in [15, 16] that, if the elastic potential W^e is a quadratic function of the logarithmic strain, i.e, a Hencky elastic potential $W^e = \frac{1}{2}\hat{\varepsilon}^e : \mathbb{D} : \hat{\varepsilon}^e$, where $\mathbb{D}$ is a fourth-order elastic tensor, the minimization results in the following explicit form for the tensor $\mathbf{M}$:

$$\mathbf{M} = \sqrt{\frac{3}{2}} \frac{\hat{\mathbf{C}}^{pr}_{n+1}}{\left\| \hat{\mathbf{C}}^{pr}_{n+1} \right\|} \, . \tag{42}$$

Having determined $\mathbf{M}$, the optimality conditions related to the variables $\Delta\alpha$ and Δd^h are evaluated in a two-step procedure. Firstly, a predictor-elastic step is tested taking $\Delta\alpha = 0$ and seeking for $\Delta d^h > 0$ that must satisfy

$$\left. \frac{\partial \mathscr{W}}{\partial \Delta d^h} \right|_{\Delta\alpha = 0^+} = 0. \tag{43}$$

Then, taking the value computed for Δd^h, it is checked the condition

$$\left. \frac{\partial \mathscr{W}}{\partial \Delta\alpha} \right|_{\Delta\alpha = 0^+} \geq 0 \, . \tag{44}$$

If the inequality is true, the minimum of $\mathscr{W}$ is attained at $\Delta\alpha = 0$ and the step is elastic-like, being $(\Delta\alpha = 0, \Delta d^h)$ the updating variables. On the other hand, if the derivative (44) results in a negative slope, then $\Delta\alpha > 0$, and a new solution for $(\Delta\alpha, \Delta d^h)$ has to be obtained in order to satisfy the stationary conditions

$$r_1 = \frac{\partial \mathscr{W}}{\partial \Delta\alpha} = \mathscr{G} \frac{\partial \hat{W}^e_{n+1}}{\partial \Delta\alpha} + \mathtt{A} + \Delta t \mathtt{B} = 0 \, , \tag{45}$$

$$\begin{aligned} r_2 = \frac{\partial \mathscr{W}}{\partial \Delta d^h} = &- \left(Y_{n+1} + g\right) + \frac{R}{\left(1 - d_{n+\theta}\right)^n \left(Y_{n+\gamma} + g\right)^{m-1}} \frac{\Delta d^h}{\Delta t} \\ &+ \Delta t \left[\theta \frac{nR}{2\left(1 - d_{n+\theta}\right)^{n+1} \left(Y_{n+\gamma} + g\right)^{m-1}} \left(\frac{\Delta d^h}{\Delta t} \right)^2 - \sigma_Y \left(\frac{\Delta\alpha}{\Delta t} \right) \right] = 0 \, , \end{aligned} \tag{46}$$

where $\mathscr{G}$, $\mathtt{A}$ and $\mathtt{B}$ are expressions given by

$$\begin{aligned} \mathscr{G} = &\left(1 - d_{n+1}\right) + \Delta t \frac{\Delta\alpha}{\Delta t} \frac{Y^S_{n+1}}{N} - \Delta t \; \sigma_Y \left(\frac{\Delta\alpha}{\Delta t} \right) S \Delta\alpha \frac{Y^{S-1}_{n+1}}{N} \\ &+ \Delta t \frac{R}{2} \left(\frac{\Delta d^h}{\Delta t} \right)^2 \gamma \frac{1 - m}{\left(1 - d_{n+\theta}\right)^n \left(Y_{n+\gamma} + g\right)^m} \\ &+ \Delta t \frac{R}{2} \left(\frac{\Delta d^h}{\Delta t} \right)^2 \theta^2 \frac{n}{\left(1 - d_{n+\theta}\right)^{n+1} \left(Y_{n+\gamma} + g\right)^{m-1}} S \Delta\alpha \frac{Y^{S-1}_{n+1}}{N} \, , \end{aligned} \tag{47}$$

$$\mathtt{A} = \mathscr{G} \kappa + \left(1 - d_{n+1}\right) \sigma_Y + f_A(\alpha_{n+1}) \left(\frac{\Delta\alpha / \Delta t}{\mathtt{c}} \right)^{\eta} \, , \tag{48}$$

$$\mathsf{B} = \frac{\mathsf{c}}{\eta+1}\left(\frac{\Delta\alpha/\Delta t}{\mathsf{c}}\right)^{\eta+1}\frac{\partial f_A(\alpha_{n+1})}{\partial\Delta\alpha} - \sigma_Y\,\frac{\Delta\alpha}{\Delta t}\frac{Y^S_{n+1}}{N} + \frac{R}{2}\left(\frac{\Delta d^h}{\Delta t}\right)^2\theta\frac{n}{(1-d_{n+\theta})^{n+1}\left(Y_{n+\gamma}+g\right)^{m-1}}\frac{Y^S_{n+1}}{N}\,. \tag{49}$$

In this work, a classical form of the free-energy plastic term $W^p(\alpha)$ is adopted, resulting into a hardening function $\kappa(\alpha)$ of Voce-like type, that is,

$$\kappa = \frac{\partial W^p}{\partial\alpha} = H\left(1-e^{-n\alpha}\right)+k\alpha\,, \tag{50}$$

where

$$W^p = H\alpha + \frac{H\left(e^{-n\alpha}-1\right)}{n} + \frac{1}{2}k\alpha^2\,, \tag{51}$$

and H, n, k are material constants. Moreover, the viscoplastic saturation $f_A(\alpha)$ is taken as a linear function of the internal variable α (i.e. a measure of accumulated plastic strain):

$$f_A(\alpha) = k_v + h\alpha\,, \tag{52}$$

being k_v and h constants. It is worth noticing that different forms of hardening and saturation functions can be proposed and easily adapted to this formulation.

Once the system has been solved, the incremental variable Δd^p is simply updated by means of (32-c), that is

$$\Delta d^p = \Delta\alpha\frac{Y^S_{n+1}}{N}.$$

By knowing the updated state of the above mentioned incremental variables, the second Piola-Kirchhoff stress is computed by means of

$$\mathbf{S}_{n+1} = 2\frac{\partial\bar{\mathscr{W}}}{\partial\mathbf{C}_{n+1}} \equiv 2\frac{\partial\mathscr{W}}{\partial\mathbf{C}_{n+1}} = \mathscr{G}\tilde{\mathbf{S}}_{n+1}\,, \tag{53}$$

where the effective stress $\tilde{\mathbf{S}}_{n+1}$ is given by the classical form

$$\tilde{\mathbf{S}}_{n+1} = 2\frac{\partial Y_{n+1}}{\partial\mathbf{C}_{n+1}} = J^{-2/3}_{n+1}\mathbb{P} : \left(2\frac{\partial W^e_{n+1}}{\partial\hat{\mathbf{C}}_{n+1}}\right) + \frac{\partial U_{n+1}}{\partial J_{n+1}}J_{n+1}\mathbf{C}^{-1}_{n+1}\,, \tag{54}$$

$$\mathbb{P} = \mathbb{I}_s - \frac{1}{3}\left(\mathbf{C}^{-1}_{n+1}\otimes\mathbf{C}_{n+1}\right)\,. \tag{55}$$

Having presented the formulation, examples of application are shown in the next section in order to evaluate some of the main potentialities of this model.

4. EXAMPLES AND RESULTS

In this section, the formulation initially proposed in [15, 16], and presented above, is employed in two numerical examples in order to analyze some of the main characteristic responses of that constitutive model. In the first case, a numerical simulation of a tensile specimen is performed. Relaxation and degradation related aspects are then observed. In the second example, a stent-like structure is tested by means of a expansion procedure, followed by an evaluation of the strength of such a structure in supporting a radial load throughout a degradation process. Comparisons between components undergoing or not degradation are also presented.

4.1 Material parameters

In an attempt to provide more realistic data for the simulations, an identification of parameters were carried out by [15, 16]. The identification procedure tried to reproduce numerically the experimental tests described by [20]. To this end, a curve fitting procedure that considered selected results published in [20] was performed. The experimental results reported in the latter were obtained by means of a series of degradation experiments on fibers of the bioabsorbable material PLLA (poly-L-lactic acid). In the current work, the data provided for tensile and relaxation tests on a non-degraded material, as well as tensile test data for nine-month degraded fibers were taken into account. The degraded fibers were tested in two conditions. In the first case, the material degrades without any load, whereas in the second test, the fibers are submitted to a constant load of 0.98 N. Assuming a mean diameter of 0.938 mm for the fibers, the identification procedure yielded the curve fitting shown in Figure 1 and the set of values presented in Table 3 [15, 16].

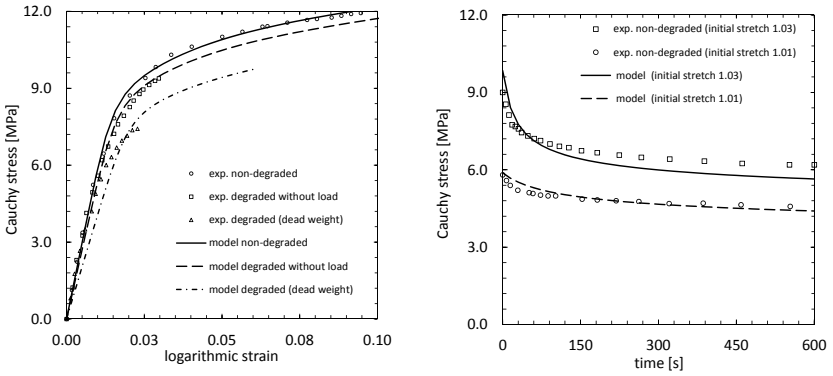

Figure 1. Curve fitting of experimental data from [20] for PLLA carried out by [15, 16]. Tensile test for non-degraded and degraded material (left). Relaxation response for a non-degraded material (right).

Table 3. Constitutive material parameters [15, 16].

Material parameter	Symbol	Value
Shear modulus (MPa)	μ	211.2676
Bulk modulus (MPa)	K	1109.155
Linear isotropic hardening modulus (MPa)	k	2
Isotropic hardening modulus (MPa)	H	2
Isotropic hardening exponent	n	50
Yield stress (MPa)	σ_Y	2.3
Viscoplasticity exponent (rate sensitive)	η	0.188
Viscoplasticity constant (viscosity, 1/s)	c	0.008
Saturation function modulus (MPa)	h	27
Saturation function constant (MPa)	k_v	10
Plastic damage exponent	S	2
Plastic damage constant $(\mathrm{J/mm^3})^S$	N	8
Hydrolytic damage exponent	m	0.3742
Hydrolytic damage exponent (damage sensitivity)	n	1
Hydrolytic damage constant $(\mathrm{J/mm^3})^{\mathrm{m}}$	R	7999.636×10^3
Hydrolytic damage constant $(\mathrm{J/mm^3})$	g	1.46×10^{-4}

Based on these constitutive parameters, we proceed with the examples.

4.2 Tests on a tensile specimen.

A simple sequence of tests was performed on a tensile specimen in order to analyze some basic characteristic responses of the constitutive model. The geometry evaluated and its dimensions are shown in Figure 2. Due to its symmetry, a finite element model was defined by considering one-eighth of the geometry. The corresponding region employed is indicated in Figure 2 by the meshed area. Two tensile tests simulate the cases in which the specimen is uniaxially deformed by means of a controlled displacement, and considering two different test velocities, that is, 0.0638 mm/s for a small deformation rate and 0.6381 mm/s for a higher rate condition. Displacement is imposed in such a way it varies linearly with time and the total deformation of the specimen will be 30 mm. Figure 3 shows the resulting reaction load vs. the variation of gage length for both cases described above.

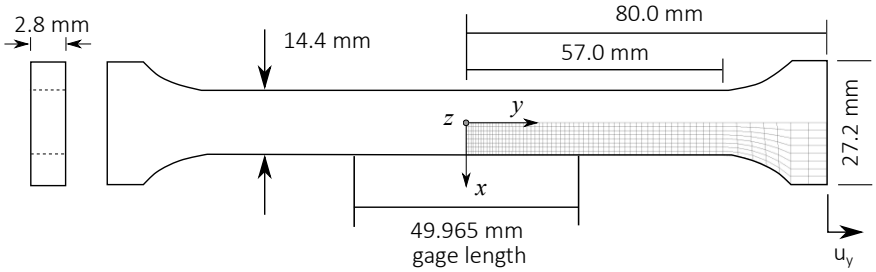

Figure 2. Geometry and dimensions of the tensile specimen.

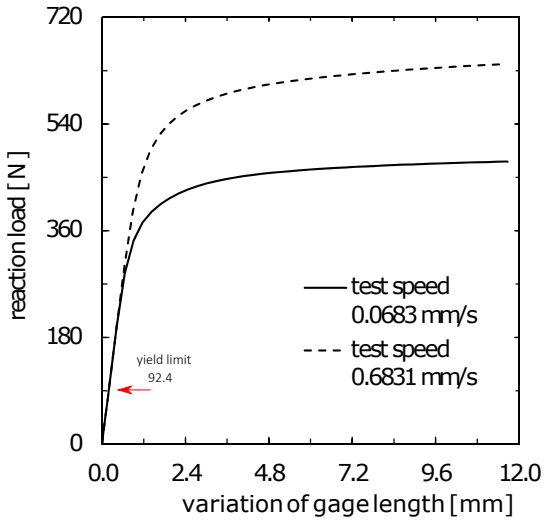

Figure 3. Reaction load vs. variation of the gage length for two deformation rates.

After this first loading step, the test continues by holding the specimen stretched (displacement boundary conditions are kept constant) over the following 600 s. By doing so, relaxation behavior is observed (after the tensile procedure) as indicated in Figure 4. Only small differences can be noticed throughout the relaxation stage for both tested conditions. In these 600 s, hydrolytic degradation is not observed due to the short period of time considered. Moreover, for this level of deformation, the ductile damage is very small, as a consequence of the values attributed to the damage constitutive parameters. In Figure 5-right, the ductile damage variables is plotted as a function of the accumulated plastic deformation. As mentioned before, the maximum ductile damage is very small for both

deformation rates. However, a typical form of relation between ductile damage and the accumulated plastic strain is noticed. Finally, as relaxation continues after this initial stage, hydrolytic degradation becomes the predominant effect and the chemical damage evolves such as indicated in Figure 5-right, achieving the value of 0.86938 in $t = 23.328 \times 10^6$ s (~ 9 months). Thus, the effects of the hydrolytic damage evolution on the stress relaxation is shown in Figure 6, where, additionally, the differences been a specimen undergoing degradation (continuous line) is compared to another one that is not affected by the hydrolysis (dashed line).

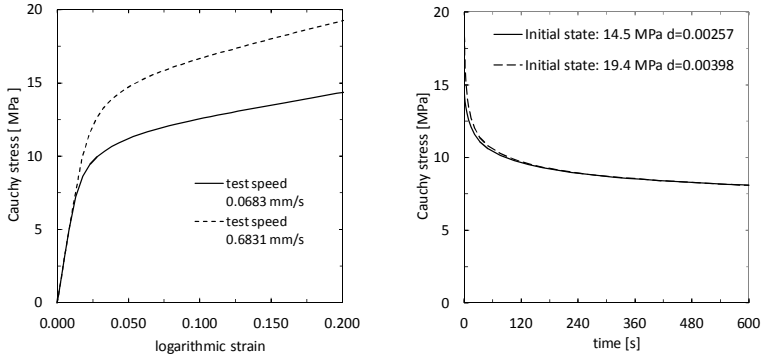

Figure 4. Cauchy stress vs. logarithmic strain curves for two deformation rates. Initial stress relaxation after tensile test (first 600 s).

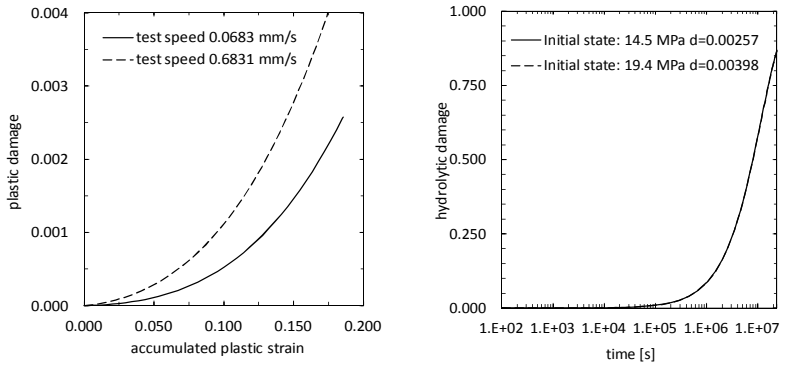

Figure 5. Ductile damage vs. accumulated plastic strain (left). Hydrolytic degradation evolution (right).

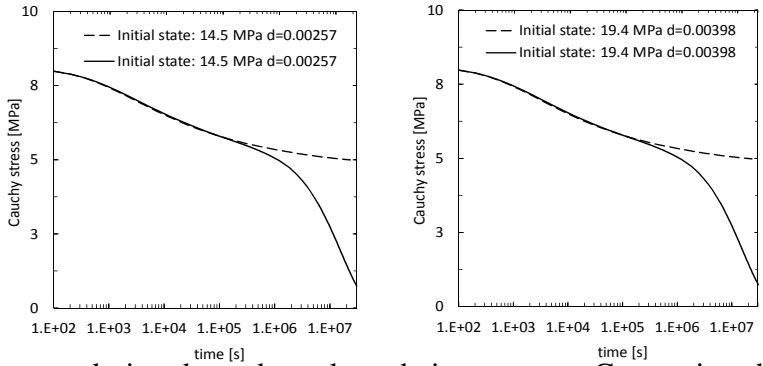

Figure 6. Cauchy stress evolution throughout degradation process. Comparison between components undergoing degradation or not.

In order to complement the analysis, the corresponding evolutions of the von Mises stress, ductile damage and the hydrolytic degradation fields that were computed for the slow-deformation procedure are shown respectively in Figures 7, 8 and 9. Quite homogeneous fields are found for the conditions simulated.

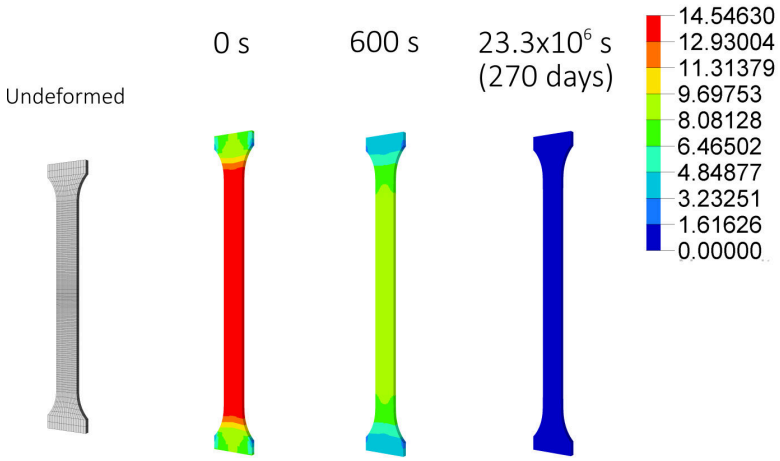

Figure 7. Evolution of von Mises stress field [MPa].

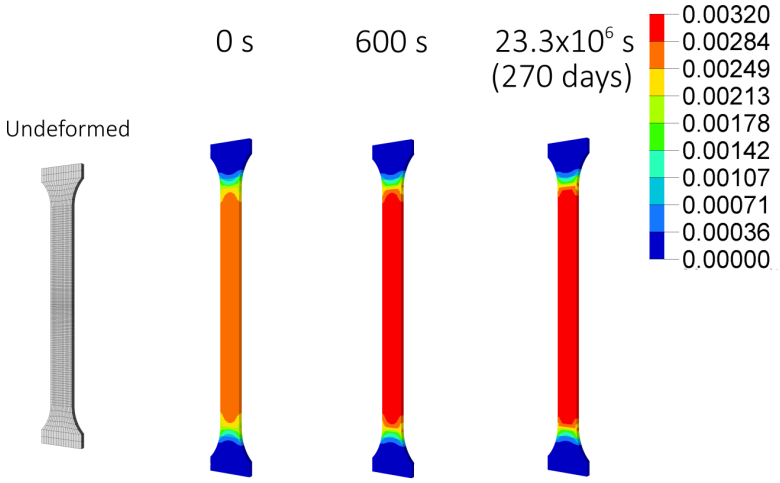

Figure 8. Evolution of ductile damage field.

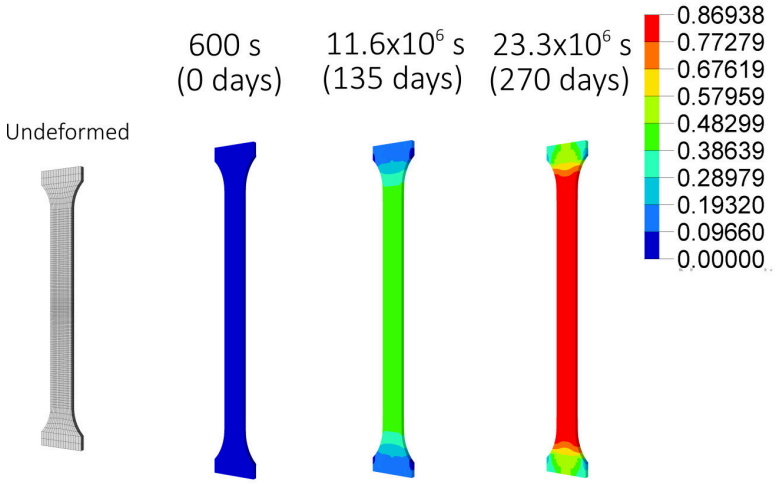

Figure 9. Evolution of hydrolytic damage field.

4.3 Tests on a stent-like frame.

As previously mentioned, bioabsorbable polymeric materials have been widely used in the design and production of medical implants such as interference screws, suture anchors, stents etc, resulting in considerable advances in trauma, orthopedic and cardiovascular procedures. Aiming at exploring the many potential applications of the constitutive formulation in discussion, a simple procedure concerning the simulation of a stent-like frame was performed.

The geometric model used in this analysis is based on one employed in the work presented by [12]. The structure has a zig-zag form with inner and outer diameters of 1.315 mm and 1.655 mm respectively (initial configuration), having the struts a mean rectangular cross section of 0.076 mm width and 0.170 mm height. The model assembly is set up by considering three parts (see Figure 10-a): the stent-like frame, an internal elastic-shell surface (representing an expansion balloon) and an external elastic-shell membrane (as an artery wall). Due to its symmetry, one-fourth of the geometry was taken into account in the finite element model, in which a mesh formed with hexahedral elements (20-nodes reduced integration) was used. The numerical experiment consists in a four-steps procedure. First, the internal shell is expanded resulting in an increase of the external diameter of the stent-like frame to 3.081 mm (Figure 10-b). During the expansion, the stent goes in contact with the external shell, whose diameter is 2.200 mm. The complete procedure takes 60 s. After this expansion step, the entire set of components is held in position for 600 s, leading to a stress relaxation process. The von Mises stress field after relaxation can be observed in Figure (11-b). This relaxation procedure aims at allowing permanent plastic deformation to take place. Then, in the third step (Figure 10-c), the balloon returns to its initial position, losing contact with the stent-like frame, while the pair stent-membrane reaches an intermediate equilibrium configuration. In such an equilibrium condition, the outer diameter of the stent-like frame is 2.287 mm, then characterizing the permanent deformation of this structure, a fact that strengthens the choice of considering a viscoplastic representation. The resulting von Mises stress field is then shown in Figure (11-c).

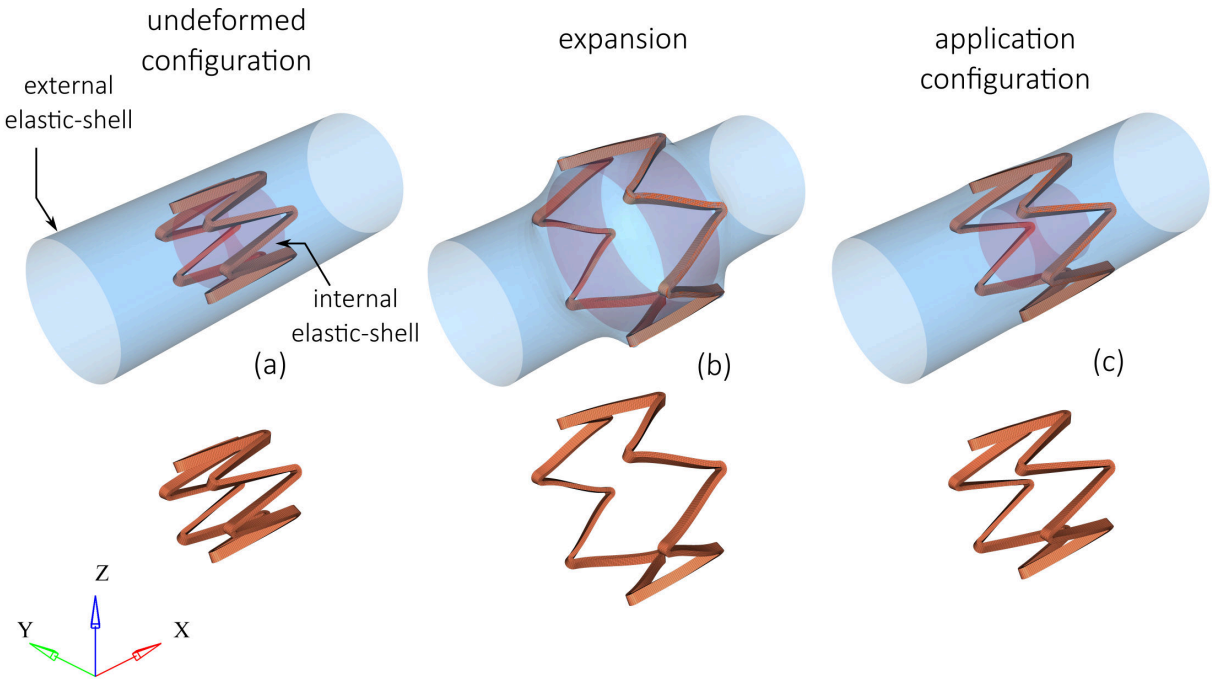

Figure 10. Geometric model and simulation stages. (a) Initial configuration. (b) Expansion step. (c) Application configuration after expansion-return procedure.

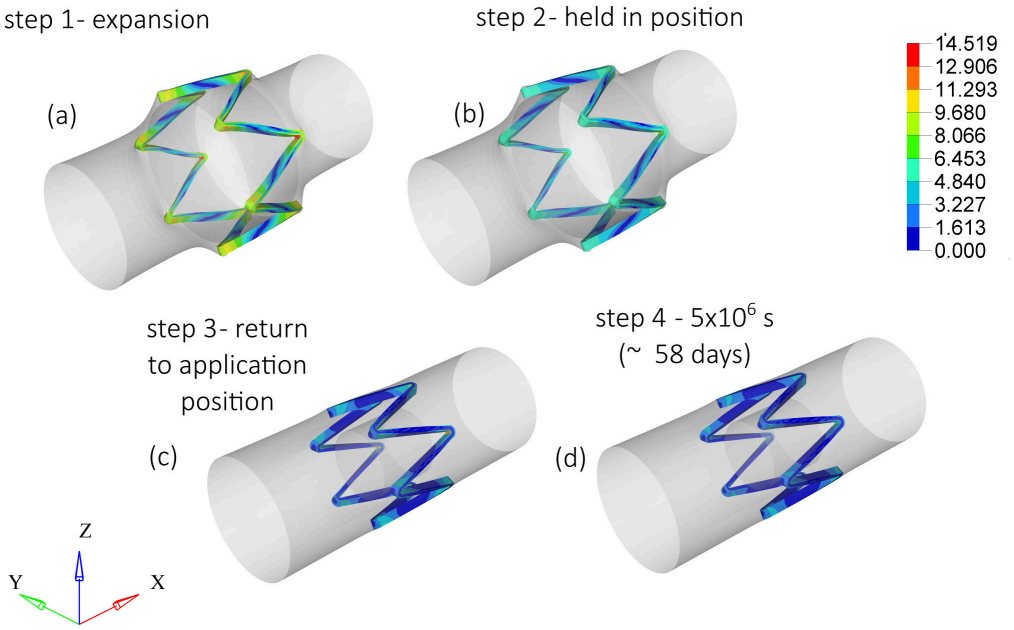

Figure 11. von Mises stress field [MPa].

Soon after the previous stage has finished, the external membrane continues to impose a radial load over the stent-like frame, and the hydrolytic degradation starts to become the prominent process. Such as in the first case analyzed (tensile specimen), the plastic damage contribution is also relatively small. The plastic damage field is presented in Figure 12, in which it is possible to see that the highest damage values occur in localized regions of the structure. This fact suggests these regions may need some special attention during the design process.

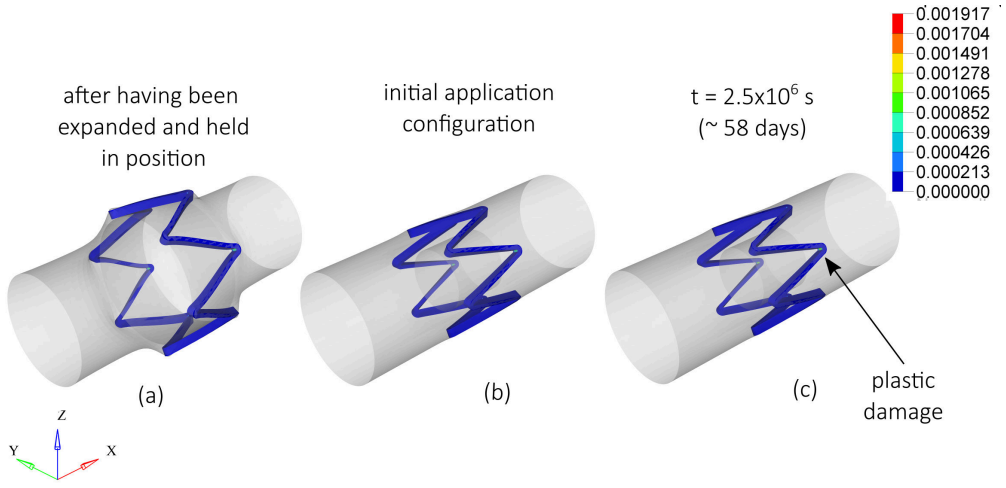

Figure 12. Evolution of the plastic-ductile damage field.

On the other hand, the chemical damage levels on the entire structure is much higher than the ductile damage, and values of $d^h = 0.34$ are found for a degradation time of 2.5×10^6 s (~ 58 days). The evolution of the hydrolytic damage field is shown in Figure 13. A major difference between models that consider deformation-induced degradation and those that do not is also made clear in Figure 13. Material in regions under higher strain levels degrades faster than those with lower ones, resulting in a non-homogeneous degradation field. Furthermore, in cases where ductile damage would have a higher contribution than this found here, viscous, ductile and chemical coupling effects would be more severe.

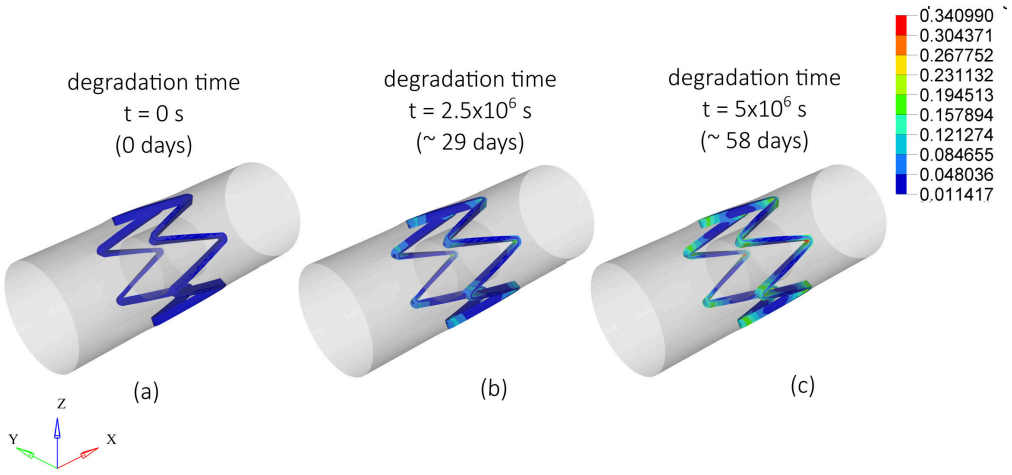

Figure 13. Evolution of the hydrolytic degradation field.

As a consequence of degradation evolution, the capacity of the structure to withstand the loading from the external shell reduces, as noticed in Figure 14. For the sake of comparison, the reduction of the normalized radial load for a component undergoing degradation (continuous line) and for another one that is not subject to hydrolysis (dashed line) are shown. This result is a clear piece of evidence sustaining the importance of taking into account degradation effects when designing products made of bioabsorbable polymers.

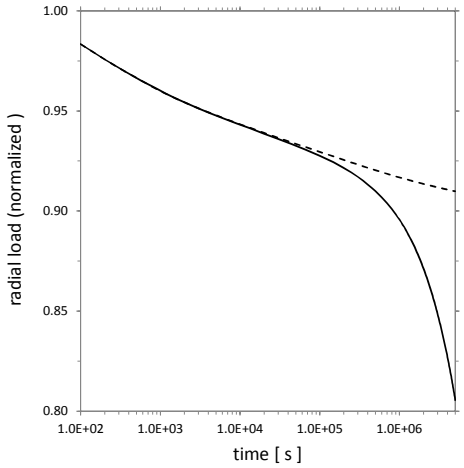

Figure 14. Reduction of the normalized radial load throughout degradation. Comparison between components undergoing degradation or not.

5. CONCLUSIONS

This paper described a constitutive model recently proposed [15, 16] in order to tackle coupling effects of elastic-viscoplasticity, ductile damage and chemical (hydrolytic) damage. The model is based on the framework of variational constitutive updates [17] and stands on consistent thermodynamic principles.

Having focused on potential applications of this constitutive formulation, some numerical tests were performed. Two different cases were evaluated. In the first one, tensile, relaxation and degradation tests were carried out for a tensile specimen. The results provided by means of experiments on the tensile specimen attested the main capabilities of the model in representing the elastic-viscoplasticity phenomenon associated with ductile-hydrolytic coupled damage. Comparisons between components

undergoing or not degradation are presented. In the second case, a stent-like structure were simulated under conditions that may resemble the deployment procedure of a stent in an artery, followed by its application condition under ductile-hydrolytic degradation. Additionally, the simulation of a stent-like frame indicates a real potential for this constitutive model to be used in the design and assessment of medical application made of bioabsorbable materials.

ACKNOWLEDGEMENTS

The authors would like to thank the Brazilian "Conselho Nacional de Desenvolvimento Científico e Tecnológico - CNPq" for supporting this research.

RESPONSIBILITY NOTICE

The author are the only responsible for the printed material included in this paper.

REFERENCES

[1] Rajagopal, K., Srinivasa, A., and Wineman, A. (2007). "On the shear and bending of a degrading polymer beam." International Journal of Plasticity, 23(9):1618 – 1636.

[2] Soares, J. S., Moore, J. E. J., and Rajagopal, K. R. (2008). "Constitutive Framework for Biodegradable Polymers with Applications to Biodegradable Stents." ASAIO Journal, 54(3):295–301.

[3] Soares, J., Rajagopal, K., and Moore, J. (2010). "Deformation-induced hydrolysis of a degradable polymeric cylindrical annulus." Biomechanics and Modeling in Mechanobiology, 9:177–186.

[4] Vieira, A., Marques, A., Guedes, R., and Tita, V. (2011). "Material model proposal for biodegradable materials." In 11th International Conference on the Mechanical Behavior of Materials, volume 10, pages 1597–1602.

[5] Vieira, A. C., Guedes, R. M., and Tita, V. (2012). "Constitutive models for biodegradable thermoplastic ropes for ligament repair." Composite Structures, 94(11):3149 – 3159.

[6] Khan, K. and El-Sayed, T. (2013). "A phenomenological constitutive model for the nonlinear viscoelastic responses of biodegradable polymers." Acta Mechanica, 224(2):287–305.

[7] Vieira, A. C., Guedes, R. M., and Tita, V. (2014). "Constitutive modeling of biodegradable polymers: Hydrolytic degradation and time-dependent behavior." International Journal of Solids and Structures, 51(5):1164–1174.

[8] Wang, Y., Pan, J., Han, X., Sinka, C., and Ding, L. (2008). "A phenomenological model for the degradation of biodegradable polymers." Biomaterials, 29(23):3393 – 3401.

[9] Rajagopal, K. R. and Muliana, A. (2009). "Shear deformation of a non-linear solid undergoing deterioration of material properties." International Journal of Structural Changes in Solids, 1(1):1–19.

[10] Muliana, A. and Rajagopal, K. (2012). "Modeling the response of nonlinear viscoelastic biodegradable polymeric stents." International Journal of Solids and Structures, 49(7-8):989–1000.

[11] Bergstrom, J. and Hayman, D. (2015). "An Overview of Mechanical Properties and Material Modeling of Polylactide (PLA) for Medical Applications." Annals of Biomedical Engineering, pages 1–11.

[12] Bobel, A., Petisco, S., Sarasua, J., Wang, W., and McHugh, P. (2015). "Computational Bench Testing to Evaluate the Short-Term Mechanical Performance of a Polymeric Stent." Cardiovascular Engineering and Technology, 6(4):519–532.

[13] Boland, E., Shine, R., Kelly, N., Sweeney, C., and McHugh, P. (2015). "A Review of Material Degradation Modelling for the Analysis and Design of Bioabsorbable Stents." Annals of Biomedical Engineering, pages 1–16.

[14] Soares, J. S. and Moore, J., James E. (2015). "Biomechanical Challenges to Polymeric Biodegradable Stents." Annals of Biomedical Engineering, pages 1–20.

[15] de Castro, P. B. (2017). Modelo de dano dúctil-hidrolítico acoplado para materiais elasto-viscoplásticos baseado em atualizações constitutivas variacionais. Tese de doutorado, POSMEC - Engenharia Mecânica, Universidade Federal de Santa Catarina, Brasil.

[16] Castro, P. B. and Fancello, E. A. "Coupled Ductile-Hydrolytic Damage Model based on Variational Constitutive Updates." Submitted to Computer Methods in Applied Mechanics and Engineering Dec. 8th, 2016.

[17] Ortiz, M. and Stainier, L. (1999). "The variational formulation of viscoplastic constitutive updates." Computer Methods in Applied Mechanics and Engineering, 171(3-4):419–444.

[18] Radovitzky, R. and Ortiz, M. (1999). "Error estimation and adaptive meshing in strongly nonlinear dynamic problems." Computer Methods in Applied Mechanics and Engineering, 172(1-4):203–240.

[19] Soares, J. S., Moore, J. E., and Rajagopal, K. R. (2007). "Theoretical Modeling of Cyclically Loaded, Biodegradable Cylinders." In F. Mollica, L. Preziosi, and K. R. Rajagopal, editors, Modeling of Biological Materials, pages 125–177. Birkhäuser Boston, Boston, MA.

[20] Soares, J. S. (2008). Constitutive Modeling of Biodegradable Polymers for Application in Endovascular Stents. Ph.D. thesis, Texas A&M University.

[21] Vieira, A., Vieira, J., Ferra, J., Magalhães, F., Guedes, R., and Marques, A. (2011). "Mechanical study of PLA-PCL fibers during in vitro degradation." Journal of the Mechanical Behavior of Biomedical Materials, 4(3):451–460.

[22] Baek, S. and Pence, T. J. (2009). "On swelling induced degradation of fiber reinforced polymers." International Journal of Engineering Science, 47(11):1100–1109.

[23] Baek, S. and Pence, T. J. (2011). "On mechanically induced degradation of fiber-reinforced hyperelastic materials." Mathematics and Mechanics of Solids, 16(4):406–434.

[24] Muliana, A., Rajagopal, K., and Subramanian, S. C. (2009). "Degradation of an Elastic Composite Cylinder due to the Diffusion of a Fluid." Journal of Composite Materials, 43(11):1225–1249.

[25] Bastos, I., Vasconcellos, J., Gomes, J., and Costa-Mattos, H. S. (2005). "A continuum damage model for the stress corrosion cracking of austenitic stainless steel." Journal of the Brazilian Society of Mechanical Sciences and Engineering, 27(2):186–191.

[26] Costa-Mattos, H. S., Bastos, I. N., and Gomes, J. A. C. P. (2008). "A simple model for slow strain rate and constant load corrosion tests of austenitic stainless steel in acid aqueous solution containing sodium chloride." Corrosion Science, 50(10):2858–2866.

[27] Costa-Mattos, H. S., Bastos, I. N., and Gomes, J. A. C. P. (2014). "A thermodynamically consistent modelling of stress corrosion tests in elasto-viscoplastic materials." Corrosion Science, 80:143–153.

[28] Grogan, J. A., O'Brien, B. J., Leen, S. B., and McHugh, P. E. (2011). "A corrosion model for bioabsorbable metallic stents." Acta Biomaterialia, 7(9):3523–3533.

[29] Gastaldi, D., Sassi, V., Petrini, L., Vedani, M., Trasatti, S., and Migliavacca, F. (2011). "Continuum damage model for bioresorbable magnesium alloy devices - Application to coronary stents." Journal of the Mechanical Behavior of Biomedical Materials, 4(3):352–365. doi: 10.1016/j.jmbbm.2010.11.003.

[30] Gurtin, M., Fried, E., and Anand, L. (2010). The Mechanics and Thermodynamics of Continua. Cambridge University Press.

[31] Lemaitre, J. (1996). A course on damage mechanics. Springer-Verlag, 2nd edition.

[32] Lemaitre, R., J. ; Desmorat (2005). Engineering damage mechanics: ductile, creep, fatigue and brittle failures. Springer-Verlag.

[33] Fancello, E. A., Lindenmeyer, L. P., Roesler, C. R., and Salmória, G. V. (2014). "A simple extension of Lemaitre's elastoplastic damage model to account for hydrolytic degradation." Latin American Journal of Solids And Structures, 11(5):884–906.

[34] Kintzel, O. and Mosler, J. (2010). "A coupled isotropic elasto-plastic damage model based on incremental minimization principles." Technische Mechanik, 30(1-3):177–184.

[35] Kintzel, O., Khan, S., and Mosler, J. (2010). "A novel isotropic quasi-brittle damage model applied to {LCF} analyses of Al2024." International Journal of Fatigue, 32(12):1948–1959.

[36] Kintzel, O. and Mosler, J. (2011). "An incremental minimization principle suitable for the analysis of low cycle fatigue in metals: A coupled ductile-brittle damage model." Computer Methods in Applied Mechanics and Engineering, 200(45-46):3127–3138.

[37] Chaboche, J. (2008). "A review of some plasticity and viscoplasticity constitutive theories." International Journal of Plasticity, 24(10):1642 – 1693. Special Issue in Honor of Jean-Louis Chaboche.

[38] Weber, G. and Anand, L. (1990). "Finite deformation constitutive equations and a time integration procedure for isotropic, hyperelastic-viscoplastic solids." Computer Methods in Applied Mechanics and Engineering, 79(2):173 – 202.

[39] Fancello, E., Ponthot, J.-P., and Stainier, L. (2006). "A variational formulation of constitutive models and updates in non-linear finite viscoelasticity." International Journal for Numerical Methods in Engineering, 65(11):1831–1864.

[40] Fancello, E., Vassoler, J., and Stainier, L. (2008). "A variational constitutive update algorithm for a set of isotropic hyperelastic-viscoplastic material models." Computer Methods in Applied Mechanics and Engineering, 197(49-50):4132–4148.